analytical chemistry

Article

pubs.acs.org/ac

Re-Electrospraying Splash-Landed Proteins and Nanoparticles

W. Henry Benner,*[,†] Gregory S. Lewis,[‡] Susanne V. Hering,[‡] Brent Selgelke,[†] Michelle Corzett,[†] James E. Evans,[§] and Felice C. Lightstone[†]

[†]Physics and Life Sciences, Biology and Biotechnology Division, Lawrence Livermore National Laboratory, P.O. Box 808, Livermore, California 94551, United States

[‡]Aerosol Dynamics, Inc., 935 Grayson Street, Berkeley, California 94710, United States

[§]Department of Molecular and Cellular Biology, University of California, Davis, Davis, California 95616, United States

Supporting Information

ABSTRACT: FITC-albumin, Lsr-F, or fluorescent polystyrene latex particles were electrosprayed from aqueous buffer and subjected to dispersion by differential electrical mobility at atmospheric pressure. A resulting narrow size cut of singly charged molecular ions or particles was passed through a condensation growth tube collector to create a flow stream of small water droplets, each carrying a single ion or particle. The droplets were splash landed (impacted) onto a solid or liquid temperature controlled surface. Small pools of droplets containing size-selected particles, FITC-albumin, or Lsr-F were recovered, re-electrosprayed, and, when analyzed a second time by differential electrical mobility, showed increased homogeneity. Transmission electron microscopy (TEM) analysis of the size-selected Lsr-F sample corroborated the mobility observation.

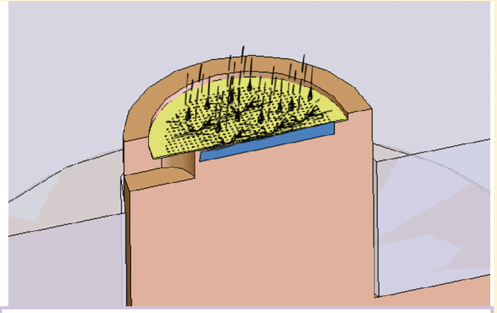

Size-selected proteins splash-landed onto a TEM grid

Publications in the field of mass spectrometry and aerosol science describe various approaches for collecting ions and particles after they have passed through a size selecting filter. In a mass spectrometer the size selecting filter is the analyzer module, and for electrical mobility separations a nano-differential mobility analyzer (nDMA) provides size selection. The aim of the investigations based on the use of a mass spectrometer has been to develop methods for collecting intact (unfragmented) ions or particles for a variety of purposes[1−6] including purification of a sample,[7] production of surface coatings,[8] studies of surface chemistry,[9,10] production of nanomaterials,[11] and preparation of a virus for TEM analysis.[12] The aim of the investigations based on deposition following electrical mobility separation has been similarly directed and includes preparation of a virus for TEM analysis[13] and the preparation of targets for X-ray diffraction studies.[14]

All of the soft landing approaches described to date using mass spectrometers provided soft landing conditions by retarding ion velocity electrostatically, thereby reducing ion energy, so that upon impact with a collection surface, ion kinetic energy is not transformed into ion internal energy and available for bond rupture. Graham Cooks' laboratory[15] introduced the concept of soft landing for ions in 1977. Their initial description focused on ions with 1−3 atoms. Since the time of the initial publication, the concept of soft landing has been refined by a number of research groups, including Cooks', with 120 articles showing up in an ISI Web of Knowledge title search of 'soft landing + ion' at the time of this writing. One of the softest approaches for landing ions was to deposit ions into thin layers of liquid.[16,17] To date, relatively small amounts of material have been deposited onto surfaces by means of soft landing due primarily to the relatively low ion currents associated with ions extracted from the analyzer section of a mass spectrometer. Working to beat this bottleneck, Mazzei et al.[9] deposited enough microperoxidase onto a surface so that voltammetry could be performed on the collected material. More notably, several investigators[18,19] deposited enough material onto a surface such that the surface could be rinsed and the recovered material analyzed by nanoESI-MS.

Soft landing has also been investigated using instruments that are not mass spectrometers, such as the work of Davila et al..[20] who collected ions after they passed through a drift tube. The physical principles defining mobility separations,[21] performed with a drift tube or DMA, are considered to be soft because the motion of an ion or charged particle in a gas is strongly influenced by aerodynamic drag, which limits ion or particle velocity to relatively low values.

In this paper we demonstrate the collection of electrosprayed protein ions or electrosprayed nanoparticles by means of a soft landing technique we call splash landing and show that it is possible to recover splash landed ions or particles and analyze them a second time using electrospray differential electrical mobility analysis. The soft landing technique we report here introduces mobility-selected ions or particles into a condensation growth tube where they accrete a coating of

Received: December 12, 2011
Accepted: January 26, 2012
Published: January 26, 2012

   dx.doi.org/10.1021/ac203298w | *Anal. Chem.* 2012, 84, 2498−2504

condensed water vapor, grow to become small droplets, and splash land onto a surface. We focus our attention on the recovery and analysis of the splash-landed material. An ion or particle residing inside of a condensation droplet is protected by the encapsulating liquid during the splash landing of the droplet, thus precluding ion fragmentation. The technique provides conditions for selecting, enriching, and collecting individual protein molecules from an initial sample consisting of multimeric forms of the protein such as small clusters of proteins or homo-oligomers. It is also demonstrated that a relatively wide size distribution of nanoparticles can be reduced to a narrow nearly monodisperse population of nanoparticles with the same technique.

EXPERIMENTAL SECTION

A summary of our approach for selecting a narrow size cut of ions or particles, collecting this material by the very soft splash landing process, recovering it, and reanalyzing it using electrospray differential electrical mobility is presented in Figure 1.

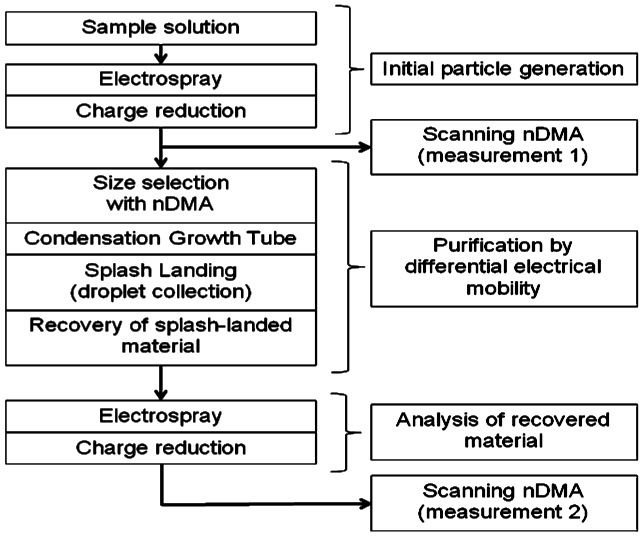

Figure 1. Overview of our experimental approach.

The differential electrical mobility instrumentation is operated in scanning mode at two points (measurement 1, measurement 2) in this scheme to acquire size distributions of the material and in fixed-mobility mode to capture size-selected material.

The experimental setup is shown in Figure 2, parts of which have been described in detail by others.[22,23] Gas-borne ions or polystyrene latex particles (PSL) were generated using an Electrospray Generator (EG, TSI, Inc., Model 3480). Liquid samples of these materials were pumped with air pressure (ΔP = 0.8 psig) through a 33 cm length of 50 μm i.d. × 220 μm o.d. of a fused silica capillary (Scientific Instrument Services, Inc., Ringoes, NJ) resulting in a sample flow of approximately 200 nL/min. The electrospray end of the capillary was mechanically abraded to form a flat-ended cone. The capillary tip was bathed in a flow of 1.5 Lpm dry air mixed with 0.25 Lpm CO_2 provided by the EG. Alpha particles from a Polonium-210 source reduced the charge on the electrospray droplets to a steady-state charge distribution characterized by the theory of Fuchs,[24] resulting a population of predominantly neutral molecules or particles, along with a small fraction that were singly charged and useful for differential electrical mobility dispersion. Charge-reduced electrospray[25] leads to ions and particles having a residue shell. The thickness of the residue is determined by the concentration of nonvolatile salts in the sample, thus diluting the sample also dilutes the salt concentration and reduces the thickness of the residue.[26] The ions or particles are nearly anhydrous[27,28] for a brief moment while they pass through a nano differential mobility analyzer (nDMA).

The differential electrical mobility instrumentation consisted of a nanodifferential mobility analyzer (nDMA, TSI, Inc. operated with a TSI, Inc. model 3080 classifier) and a condensation particle counter (CPC; TSI, Inc., model 3025). The flow of gas through each of these components was decoupled (excess gas allowed to escape) from the overall system so that each could be operated independently. The differential electrical mobility instrumentation was operated in scanning mode to measure particle size distributions ranging from 2 to 72 nm or in fixed-mobility mode to collect size-selected ions. Further details of the analysis system are presented in the Supporting Information.

The CGTC in Figure 2 (Aerosol Dynamics, Inc., Berkeley, CA) is basically a device that operates on the principle of a CPC with the provision that the condensation droplets do not pass through a droplet-counting detector and instead are directed through nozzles that accelerate the condensation droplets toward a surface, causing them to be collected via splash impaction. Air carrying ions or particles enter three fine mesh tubes (two are shown in the drawing), each having an entrance section that is cooled and a second section that is warmed. The mesh tubes are wetted with water and serve to introduce water vapor into the transiting air stream. The growth tube operates on principles identified by Hering et al.[29,30] In our experiments, 1 Lpm of air is divided among three 1/4″ id mesh tubes in the CGTC, each of which connects to a 0.03″ diameter tubular nozzle. The temperature at the entrance to the mesh tubes was set to 8 °C, while the second sections of the mesh tubes were operated at 30 °C. The nozzles act as a transition zone between the mesh tubes and an impactor chamber operated at 30 °C or slightly higher.

Splash landing is a type of impaction technique used by the aerosol science community to collect liquid and solid aerosols on a surface. As the jet of gas-borne droplets spreads and flows over the collection surface, the droplets fail to follow the gas streamlines[31] and impact (splash land) onto the surface by centrifugal force where they accumulate. Selection of appropriately sized nozzles (0.03″ id) based on gas flow (1 Lpm), along with the spacing between the nozzle and the impactor surface (0.1″), provides an efficient way to collect the droplets (1−3 μm diameter) generated in the condensation growth tube. Two types of impactors were used to splash land droplets. The first, shown in the left panel of Figure 3 aimed a jet of droplet-laden air at a flat glass surface (circular microscope coverslip derivatized with Aqua-sil, Pierce Biotechnology) secured in place with heat transfer paste onto the top of a short pedestal in a temperature controlled stainless steel chamber. The chamber and impactor surface were heated to 30 °C, a temperature derived experimentally that was not too warm to evaporate the splash landed droplets nor too cool to condense water vapor onto the surface.

A second type of impactor used in this study (right panel, Figure 3) was designed to provide longer unattended operation so that larger quantities of a protein could be collected. Here a

dx.doi.org/10.1021/ac203298w | Anal. Chem. 2012, 84, 2498−2504

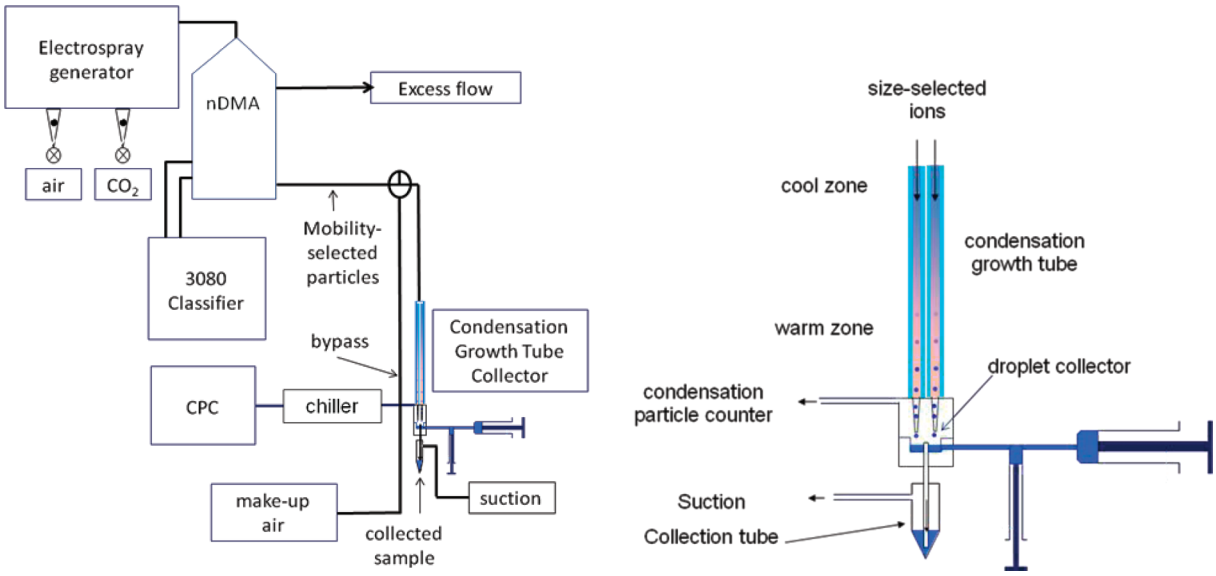

Figure 2. Experimental setup. nDMA = nanodifferential mobility analyzer, CGTC = condensation growth tube collector, CPC = condensation particle counter. The chiller reduced the amount of water vapor entering the butanol-based CPC. The right panel shows an enlarged view of the CGTC.

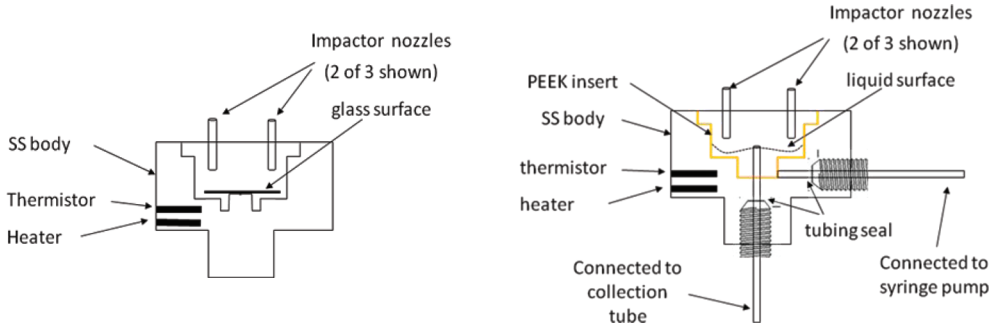

Figure 3. Impactors showing glass coverslip (derivatized with Aqua-sil (left) onto which droplets are impacted or into a small pool of liquid (right), where it can be seen that the jets of gas depress the liquid.

100 μL cup-shaped device fabricated from PEEK was pressed into a stainless steel housing and when filled with liquid provided a liquid surface for collecting splash landed droplets. Ports provided a means for adding and withdrawing liquid. A 1 mL syringe (manually operated) and a 25 mL syringe (operated with a syringe pump) were used to adjust the amount of liquid in the cup (refer to Figure 2, right). A small diameter tube, attached to a collection tube and a source of suction, extended up through the bottom of the cup to a height that maintained a predetermined volume (typically 100 μL) in the bottom of the cup. The air stream passing from the impactor to the CPC was nearly saturated with water vapor. If this water vapor was allowed to enter the CPC, it would have been absorbed by the butanol in the condenser tube inside the CPC and reduced the CPC's detection efficiency. To prevent this problem, a small thermoelectric cooler was used to chill a 10″ length of metal tubing on the inlet to the CPC, which removed a majority of the water vapor via water vapor condensation.

MATERIALS

FITC-albumin (PN: A 9771) was purchased from Sigma Chemical and diluted with 25 mM aq. ammonium acetate. 0.02 μm diameter particles (PN: F8787, Fluorospheres) were purchased from Invitrogen and diluted with 25 mM aq. ammonium acetate. The Lsr-f was prepared via a cloning procedure described in the Supporting Information. The transmission electron microscope (TEM) samples were prepared with TEM grids coated with amorphous carbon and then stained with uranyl formate using procedures described in the Supporting Information.

RESULTS

A critical parameter for forcing water to condense onto ions and nanoparticles is the difference in temperature between the cooled and heated zones along the growth tube in the CGTC. It can be understood that when the temperature difference (ΔT) between the cooled and heated zones is larger, larger droplets form and vice versa when the temperature difference is smaller. Larger droplets are collected by impaction more efficiently than smaller droplets. Droplet size measurements were obtained by drawing the droplets into an aerodynamic particle sizer (TSI, INC., model 3321) and recording droplet size distributions as a function of ΔT. The droplet size distribution extended from 1.8 to 3.2 μm and peaked at 2.64 μm. The efficiency with which nanoparticles and protein ions are transformed into condensation droplets is also important to understand because it governs the overall collection efficiency.

dx.doi.org/10.1021/ac203298w | *Anal. Chem.* 2012, 84, 2498–2504

The collection efficiency was 98.5% at 7.7 nm, 99.5% at 10 nm, 99.8% at 12 nm, and 100% for particles larger than 15 nm.

The temperatures of each zone cycled from a set point temperature to about 2 degrees above the set point, which led to small variations in the conditions causing droplet formation as detected by variations in the number concentration of particles detected downstream of the droplet impactor. These variations were insubstantial (± approximately 0.1%) in terms of altering ion or particle collection efficiency.

The droplets exiting the CGTC had an average diameter of 2.64 μm and equivalent to a volume of 9.2×10^{-12} cm^3. When 1×10^5 ions/cm^3, a typical input concentration to the CGTC, pass through the CGTC at 1 Lpm, approximately 1 μL/min of droplets are collected. This volumetric collection rate for droplets is negligible in comparison to the 100 μL of starting buffer in the collection cup and did not substantially dilute the buffer during droplet collection.

Conditions for operating the CGTC were optimized by electrospraying nominally 0.02 μm diameter fluorospheres, which range in size from about 15 to 50 nm, from which a narrow size cut was selected using differential electrical mobility and recovered via splash landing. In order to understand the filtering efficiency of our size-selecting process, it was important to characterize the starting material and then compare it to the size-selected material. The blue line in Figure 4 shows the size

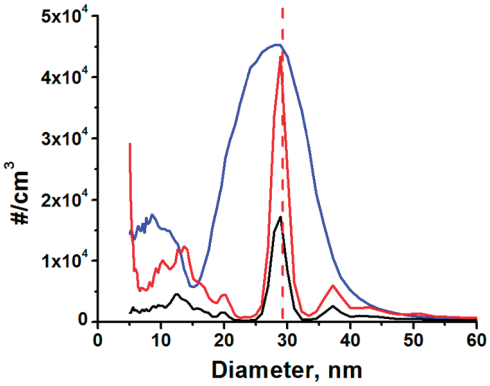

Figure 4. Size distributions of fluorospheres. Blue = 1/4 dil of 0.02 nm fluorospheres from which size-selected (29 nm, red dashed line) particles were collected, red = recovered 29 nm size-selected fluorospheres, black = 1/3 dil of 29 nm size-selected fluorospheres showing a small shift toward smaller diameter. The width of the dashed line does not represent the resolving power of the nDMA.

distribution of the nominally 0.02 μm particles, obtained using measurement 1 in Figure 1. The modal diameter is 29.4 nm when the particles were diluted 1/4 and 28.8 nm (not shown) when they were diluted 1/4000. Further dilutions of the particles did not substantially shift the modal diameter of the particles to smaller sizes. The difference between the two modal diameters is caused by the presence of surfactant in the stock solution of the particles. A broad peak at 7 nm for the 1/4 dilution of particles corresponds to residue particles of the surfactant. When the 1/4 dilution of particles is electrosprayed, the dry particles carry a coating of the dry surfactant, which shifts the measured size from 28.8 to 29.4 nm.

The vertical red dashed line in Figure 4 at 29 nm represents the diameter of particles that were targeted for size selection. The nDMA nominally operates with a resolving power between 10 and 20 (depends on sheath flow rate), which means that particles slightly smaller and slightly larger than 29 nm will be size-selected simultaneously. The nDMA was set to 29 nm and operated in fixed-mobility mode for 1000 min and ~70 μL, slightly less than predicted, of droplets were collected. The collected liquid was removed with a pipet, transferred to a 1.5 mL microcentrifuge tube, and evaporated to about 20 μL under a jet of filtered air. Following addition of 2 μL of 250 mM ammonium acetate, the recovered solution was re-electrosprayed and analyzed by nDMA operated in scanning mode.

The size distribution of the splash landed size-selected particles, obtained using measurement 2 in Figure 1, is represented by the red plot in Figure 4. It is characterized by a dominant peak centered at 28.8 nm with fwhm equal to 2.7 nm. The modal diameter of the recovered material is slightly smaller than the diameter dialed into the nDMA's controller, and the observed shift in diameter from 29 to 28.8 nm can be attributed to the presence of surfactant in the initial particle solution. As the size-selected particles are collected they become diluted by the condensed water they accreted while passing through the CGTC. When re-electrosprayed, they carry a thinner residue of surfactant and emerge in the spectrum as a peak centered at 28.8 nm. Upon further dilution of the collected material by 1/3, the measured particle size is shifted further toward smaller diameter (28.7 nm), displayed as the black plot in Figure 4, again as a result of a lower surfactant concentration. The spectrum of the splash landed size-selected particles also has small peaks at 20 nm, 37 nm, and 42 nm. An explanation for the peak at 20 nm is not concrete - it may be partially due to the production of doubly charged 29 nm particles that result from the charge reduction process when 29 nm particles are electrosprayed, since 29 nm particles at +2 have the same electrical mobility as 20 nm particles at +1.[32] The peaks at 37 and 42 nm appear to comprise doublets and triplets of 29 nm particles, which could have formed after collection because there is no longer any surfactant in the solution to prevent the size-selected particles from clumping. The heights of these peaks, relative to the height of the 29 nm peak, approximates the distribution of dimers and trimers predicted by Poisson statistics.

nDMA spectra of several concentrations of FITC-albumin (0.01, 0.1, and 1 mg/mL), presented in Figure 5, are characterized by a peak at 7.1 nm that corresponds to the monomeric form of FITC-albumin, and additional peaks corresponding to multimeric forms of FITC-albumin. When FITC-albumin is electrosprayed at 0.01 mg/mL (green plot), the monomeric form at 7.1 nm dominates a small peak at 8.8 nm representing the dimeric form.

Further dilution of the FITC-albumin did not shift the location of the peaks in the spectrum and therefore it can be concluded that the peak at 7.1 nm represents the size of single molecules of FITC-albumin. At the highest concentration of FITC-albumin (1 mg/mL) a wide peak (blue plot in Figure 5) centered at about 13 nm represents a distribution of particles carrying 2–20 FITC albumin molecules. The primary electrospray droplets were approximately 250 nm in diameter, as determined by sucrose residue particle measurements[26] and results in the production of approximately 1.2×10^{14} droplets after 1 cm^3 of sample is electrosprayed. If every one of these droplets contained a single FITC-albumin molecule the albumin concentration would have been 2×10^{-7} M or 0.013 mg/mL. One of the concentrations of FITC-albumin used to generate the plot in Figure 5 was 0.01 mg/mL, approximately the concentration that would produce droplets containing a single molecule of FITC-albumin on average.

dx.doi.org/10.1021/ac203298w | Anal. Chem. 2012, 84, 2498–2504

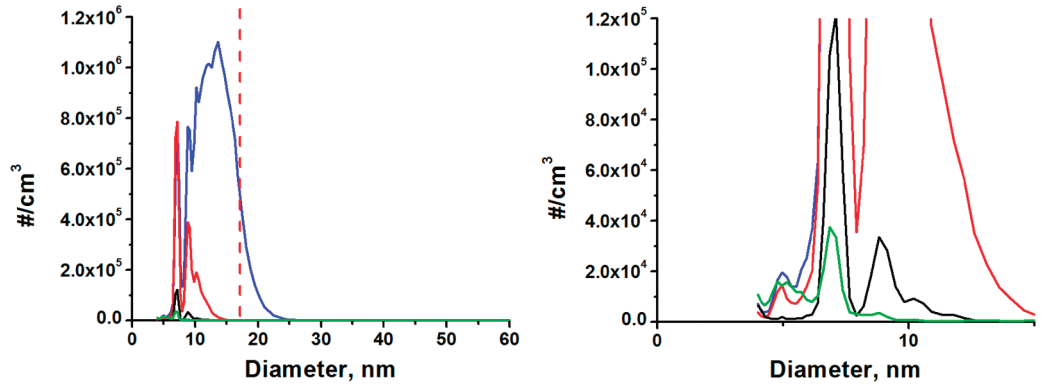

Figure 5. Size distribution of FITC-albumin samples. Blue = 1 mg/mL FITC-albumin from which size-selected (17 nm, red dashed line) albumin particles were collected, black = 0.1 mg/mL FITC-albumin, green = 0.01 mg/mL FITC-albumin, red = recovered size-selected albumin particles after dissolution. The right panel is an expanded view of the left panel.

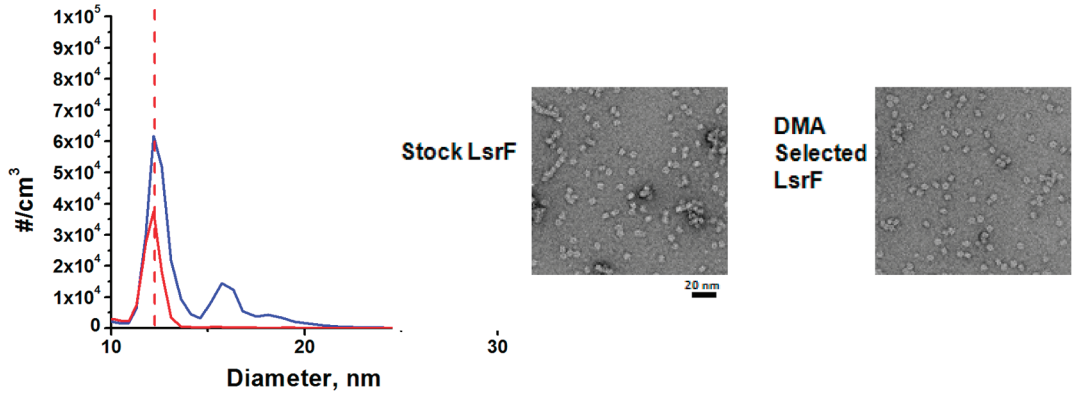

Figure 6. Left panel: Size distributions of Lsr-f samples. Blue = 1/50 dilution of stock Lsr-F (scaled by counts/20 for the purpose of revealing the relative peak positions) from which size-selected (12.2 nm, red dashed line) particles were collected, red = recovered size-selected Lsr-F after concentrating and dialyzing the collected material. Right panel: Negatively stained TEM images of LSR-F before (left) and after (right) purification by means of size-selecting differential mobility separation and collection by means of splash landing. Magnification bar represents 20 nm for both images.

Poisson statistics predicts that the probability of two molecules per droplet is 0.18 when the concentration of FITC-albumin is 0.01 mg/mL. The ratio of monomer (7.1 nm) peak height to dimer (8.8 nm) peak height for the 0.01 mg/mL sample was 0.27, somewhat larger than 0.18, presumably to the fact that albumin homodimers form in solution and artificially boost the ratio above that predicted by Poisson statistics. The fact that homodimers are present in this sample is substantiated by the fact that all dilutions of FITC-albumin, including 0.001 mg/mL, near the limit of detection and not shown, have a peak at 8.8 nm in nDMA spectra, which should have disappeared if Poisson statistics were applicable.

For the purpose of splash landing condensation droplets carrying FITC-albumin molecules, the differential mobility instrumentation was operated in fixed-mobility mode, and the nDMA was set to transmit 17 nm diameter particles of FITC-albumin to the CGTC. A 17 nm FITC-albumin particle contains 15 FITC-albumin molecules, as determined from the volume of a single FITC-albumin molecule having a measured diameter of 7.1 nm. The optimal operating conditions for the CGTC were to set the cooled zone to 8 °C, the heated zone to 30 °C, and the collection cup to 25 or 30 °C. One Lpm of gas flowing through the CGTC was a factory design parameter and used by default. Droplets containing 17 nm particles of FITC-albumin were splash landed for several hours resulting in the accumulation of three small beads of liquid that formed on the coverslip directly underneath each of the three nozzles in the impactor. This volume was highly fluorescent when examined with an epi-fluorescence microscope microscope. Splash landing of condensation droplets carrying 17 nm particles of FITC-albumin was continued overnight and combined with the material collected for several hours initially. The liquid that accumulated on the coverslip was recovered and analyzed by electrospray nDMA. The size distribution of size-selected FITC-albumin is shown as the red plot in Figure 5. This spectrum is the result of collecting 17 nm particles of FITC-albumin, which, upon accumulation in a pool of splash landed droplets, dissolve and convert predominantly to the monomeric state. Expansion of the red plot (not shown) reveals that a small fraction of the FITC-albumin appears in a peak at 8.8 nm and indicates that the homodimer of FITC-albumin also reforms.

The splash landing process was also used to collect size-selected Lsr-F. Stock material of Lsr-F was diluted 1/50 with 25 mM ammonium acetate, then electrosprayed, and analyzed by nDMA. The size distribution of the material is shown in Figure 6. It is characterized by a peak at 12.2 nm, corresponding to the monomeric form and a smaller peak at 15.8 nm, corresponding presumably to the dimeric form. The size distribution stretches to the upper limit of the scan (72 nm), although very little material is detected above about 30 nm. The differential mobility instrumentation was then operated in fixed-mobility mode and set to transmit 12.2 nm ions of Lsr-F to the CGTC.

dx.doi.org/10.1021/ac203298w | *Anal. Chem.* 2012, 84, 2498–2504

By setting the nDMA to transmit 12.2 nm ions, ions corresponding to debris (Dp > 15 nm) and dimers and trimers were excluded.

Droplets containing monomeric Lsr-F were splash landed overnight using the second type of impactor, into which 100 μL of 250 mM ammonium acetate was placed at the start of collection. During the overnight collection, 590 μL of liquid was accumulated in the collection vial, therefore along with the 100 μL remaining in the impactor, the 250 mM buffer was diluted by a factor of 100/690, to 36 mM. This size-selected material was concentrated by evaporation under a jet of filtered air to 20 μL and then drop dialyzed against 25 mM ammonium acetate for 1 h. The size distribution of the recovered size-selected Lsr-F is represented by the red plot in Figure 6.

The droplet collection times used in this study were long because analysis by electrospray differential electrical mobility has a detection limit of about 1 μg/mL for proteins due to the nature of charge-reduced electrospray. For example, only about 15% of 29 nm particles carry one charge and are useful for analysis. The fraction of +1 charged ions is even smaller for the proteins we studied.

Eight μL aliquots of Lsr-F of a 1/100 dilution of Lsr-F starting material or monomeric size-selected Lsr-F were adsorbed to separate TEM grids. The grids were processed by negative staining (see the Supporting Information) and examined using TEM. Images of the two samples are shown in Figure 6, right panel. LSr-F macromolecules are arranged as a decamer with two rings of pentamers and have a diameter of 10.5 nm and a height of 6.6 nm. The diluted starting material shows aggregated chains of Lsr-F macromolecules along with monomers, dimers, trimers, and larger clumps of Lsr-F macromolecules. Approximately 15% of the Lsr-F molecules are monomers, and the remainder is aggregated. The size-selected sample of monomeric Lsr-F shows a few small clumped particles, but chains and large clumps are no longer observed. In the size-selected sample, approximately 70% of the Lsr-F molecules are in the monomeric form. Since the adsorption and staining procedures were identical for both samples, any potential artifacts from incubation with a heavy metal salt solution (uranyl formate) or interaction with the partially charged carbon film should be identical. Thus, the TEM results indicate the size-selection process creates a more homogeneous population of molecules.

CONCLUSIONS AND FUTURE DIRECTIONS

We have demonstrated that the use of differential electrical mobility instrumentation, in conjunction with a condensation growth tube collector, and the splash landing process can be used to process and purify nanoparticles and biological samples. The approach provides a way to size-select small quantities of these materials out of a more complicated mixture for subsequent testing or analysis. We have demonstrated that a distribution of nanoparticles, initially having fwhm of 17 nm (extending from 18 to 35 nm), can be processed to produce a population of particles that is nearly monodisperse with a fwhm of 2.7 nm. Any size of fluorospheres between 15 and 45 nm could have been selected from the nominally 0.02 μm diameter starting material. The same capability was also demonstrated with FITC-albumin and Lsr-F proteins.

One application of the technique reported here is to use it to prepare more homogeneous populations of macromolecules for TEM or cryo-electron microscopy (cryo-EM) analysis. Liquid samples are typically prepared for TEM or cryo-EM by placing a small drop (5−10 μL) of sample onto a high surface tension surface onto which a TEM grid is carefully dropped. The splash landing technique described here should make it possible to start with a droplet of buffer atop a TEM grid and then bombard the grid with droplets of size-selected material until an adequate quantity of sample is accumulated on the wet grid similar to the way samples are collected for time-resolved cryo-EM.[33] The grid can then be further processed for TEM or cryo-EM inspection using standard procedures.

It is understandable that there may be concern for the stability of a protein ion during the process of drying an electrospray droplet. It is possible to consider an experimental design that begins with electrospraying a protein using a dilute nonvolatile buffer in addition to our use of 25 mM AA so that the dry protein ion carries with it a thin residue of buffer. The presence of nonvolatile buffers in electrospray samples can cause an electrospray to be unstable or not work at all, but careful tuning of the buffer concentration leads to success[34−36] and has been used to stabilize proteins. Adding a nonvolatile buffer will necessitate understanding how much the diameter is shifted by the residue shell so that it can be size-selected. Another approach would be to coat the impactor surface with a residue of buffer so that the impacted droplets will pick up buffering capacity when the buffer dissolves in the collection of droplets.

Many nanoparticles are characterized by broad size distributions such as the distribution shown in Figure 4 for 0.02 μm fluorospheres. Sources of nearly monodisperse nanoparticles are needed for calibrating particle sizing instruments and high molecular weight samples that have been separated by means of gradient gel electrophoresis. The production of small quantities of nearly monodisperse particle standards[37] appears to be attainable with the methods described in this paper.

ASSOCIATED CONTENT

Supporting Information

Additional details about the preparation of sample material, performance of the condensation growth tube collector (CGTC), sample analysis, and improvements. This material is available free of charge via the Internet at http://pubs.acs.org.

AUTHOR INFORMATION

Corresponding Author

*E-mail: benner2@llnl.gov.

Notes

The authors declare no competing financial interest.

REFERENCES

(1) Peng, W.-P.; Goodwin, M. P.; Nie, Z.; Volny, M.; Ouyang, Z.; Cooks, R. G. *Anal. Chem.* **2008**, *80*, 6640−6649.

(2) Gologan, B.; Green, J. R; Alvarez, J.; Laskin, J.; Cooks, R. G. *Phys. Chem. Chem. Phys.* **2005**, *7*, 1490−1500.

(3) Volny, M.; Elam, W. T.; Branca, A.; Ratner, B. D.; Turecek, F. *Anal. Chem.* **2005**, *77*, 4890−4896.

(4) Hadjar, O.; Futrell, J. H.; Laskin, J. *J. Phys. Chem.* **2007**, *111*, 18220−18225.

(5) Rauschenbach, S.; Vogelgesang, R.; Malinowski, N.; Gerlach, J. W.; Benyoucef, M.; Costantini, G.; Deng, Z.; Thontasen, N.; Kern, K. *ACS Nano* **2009**, No. 3, 2901−2910.

(6) Benesch, J. L. P.; Ruotolo, B. T.; Simmons, D. A.; Barrera, N. P.; Morgner, N.; Wamg, L.; Saibil, H. R.; Robinson, C. V. *J. Struct. Biol.* **2010**, *172*, 161−168.

(7) Mayer, P.; Turecek, F.; Lee, H.; Scheidmann, A.; Lney, T.; Schumacher, F.; Strop, P.; Smrcina, M.; Patek, M.; Schirlin, D. *Anal. Chem.* **2005**, *77*, 4378−4384.
(8) Hanley, L.; Sinnott, S. B. *Surf. Sci.* **2002**, *500*, 500−522.
(9) Mazzei, F.; Favero, G.; Frasconi, M.; Tata, A.; Tuccitto, N.; Licciardello, A.; Pepe, F. *Anal. Chem.* **2008**, *80*, 5937−5944.
(10) Hadjar, O.; Wang, P.; Futrell, J. H.; Dessiaterik, Y.; Zhu, Z.; Cowin, J. P.; Iedema, M. J.; Laskin, J. *Anal. Chem.* **2007**, *79*, 6566−6574.
(11) Nagaoka, S.; Matsumoto, T.; Ikemoto, K.; Mitsui, M.; Nakajima, A. *J. Am. Chem. Soc.* **2007**, *129*, 1528−1529.
(12) Siuzdak, G.; Bothner, B.; Yeager, M.; Brugidou, C.; Fauquet, C. M.; Hoey, K.; Chang, C. M. *Chem. Biol.* **1996**, *3*, 45−48.
(13) Allmaier, G.; Laschober, C.; Szymanski, W. W. *J. Am. Soc. Mass Spectrom.* **2008**, *19* (8), 1062−1068.
(14) Bogan, M. J.; Benner, W. H.; Hau-Riege, S. P.; Chapman, H. N.; Frank, M. *J. Aerosol Sci.* **2008**, *29*, 917−928.
(15) Franchetti, V.; Solka, B. H.; Baitinger, W. E.; Amy, J. W.; Cooks, R. G. *Int. J. Mass Spectrom. Ion Phys.* **1977**, *23* (1), 29−35.
(16) Gologan, B.; Green, J. R.; Alvarez, J.; Laskin, J.; Cooks, R. G. *Phys. Chem. Chem. Phys.* **2005**, *7*, 1490−1500.
(17) Gologan, B.; Takats, Z.; Alvarez, J.; Wiseman, J. M.; Talaty, N.; Ouyang, Z.; Cooks, R. G. *Anal. Chem.* **2004**, *15*, 1874−1884.
(18) Badu-Tawiah, A. K.; Wu, C.; Cooks, R. G. *Anal. Chem.* **2011**, *83*, 2648−2654.
(19) Yang, X.; Mayer, P. S.; Turecek, F. *J. Mass Spectrom.* **2006**, *41*, 256−262.
(20) Davila, S. J.; Birdwell, D. O.; Verbeck, G. F. *Rev. Sci. Instrum.* **2010**, *81*, 3 DOI: 10.1063/1.3361041.
(21) Revercomb, H. E.; Mason, E. A. *Anal. Chem.* **1975**, *47*, 970−983.
(22) Kaufman, S. L.; Skogen, J. W.; Dorman, F. D.; Zarrin, F. *Anal. Chem.* **1996**, *68*, 1895−1904.
(23) Kaddis, C. S.; Lomeli, S. H.; Yin, S.; Berhane, B.; Apostol, M. I.; Kickhoefer, V. A.; Rome, L. H.; Loo, J. A. *J. Am. Soc. Mass Spectrom.* **2007**, *18*, 1206−1216.
(24) Fuchs, N. A. *Geofis. Pura Appl.* **1963**, *56*, 185−193.
(25) Bacher, G.; Szymanski, W. W.; Kaufman, S. L.; Zollner, P.; Blass, D.; Allmaier, G. *J. Mass Spectrom.* **2001**, *36*, 1038−1052.
(26) Kaufman, S. L. *J. Aerosol Sci.* **1998**, *29*, 537−552.
(27) Hoaglund-Hyzer, C. S.; Counterman, A. E.; Clemmer, D. E. *Chem. Rev.* **1999**, *99*, 3037−3079.
(28) Jarrold, M. F. *Annu. Rev. Phys. Chem.* **2000**, *51*, 179−207.
(29) Hering, S. V.; Stolzenburg, M. R. *Aerosol Sci. Technol.* **2005**, *39*, 428−436.
(30) Hering, S. V.; Stolzenburg, M. R.; Quant, F. R.; Oberreit, D. R.; Keady, P. B. *Aerosol Sci. Technol.* **2005**, *39* (7), 659−672.
(31) Aerosol Technology, W. C. Hinds, Wiley-Interscience: 1982; p 114.
(32) TSI, Inc., Model 3986 SMPS Operator's manual.
(33) Lu, Z.; Shaikh, T. R.; Barnard, D.; Meng, X.; Mohamed, H.; Yasin, A.; Mannella, C. A.; Agrawal, R. K.; Lu, T.-M.; Wagenknecht, T. *J. Struct. Biol.* **2009**, *168*, 388−395.
(34) Chen, C. H.; Emond, M. H. J.; Kelder, E. M.; Meester, B.; Schoonman, J. *J. Aerosol Sci.* **1999**, *30* (7), 959−967.
(35) Widiyandari, H.; Hogan, C. J.; Yun, K. M.; Iskandar, F.; Biswas, P.; Okuyama, K. *Macromol. Mater. Eng.* **2007**, *292* (4), 495−502.
(36) Freeke, J.; Robinson, C. V.; Ruotolo, B. T. *Int. J. Mass Spectrom.* **2010**, *298*, 91−98.
(37) Ude, S.; de la Mora, J. F.; Alexander, J. N. IV; Saucy, D. A. *J. Colloid Interface Sci.* **2006**, *293*, 384−393.